

Observation of Nonmagnetic Resonant Scattering Effects by Tunneling in Dilute Al-Mn Alloy Superconductors

G. O'Neil,^{1,2} D. Schmidt,¹ N. A. Miller,^{1,2} J. N. Ullom,¹ A. Williams,³ G. B. Arnold,³ and S. T. Ruggiero³

¹National Institute of Standards and Technology, 325 Broadway, Boulder, Colorado 80305, USA

²Department of Physics, University of Colorado, Boulder, Colorado 80309, USA

³Department of Physics, University of Notre Dame, Notre Dame, Indiana 46556, USA

(Received 29 June 2005; revised manuscript received 24 October 2007; published 6 February 2008)

We have observed the BCS-like density of states predicted for energy-gap suppression by nonmagnetic Anderson impurities in superconductors. We show that Mn impurities in Al exhibit no magnetic character and act exclusively as strong resonant scattering sites without producing time-reverse symmetry breaking of Cooper pairs (pair breaking).

DOI: [10.1103/PhysRevLett.100.056804](https://doi.org/10.1103/PhysRevLett.100.056804)

PACS numbers: 74.50.+r, 73.40.Gk, 74.70.Ad

The understanding of a wide range of condensed-matter phenomena is replete with insightful studies of impurity-induced and -stabilized phenomena. This includes systems near quantum critical points where the survival of one type of order is governed by scattering effects [1]. While studies of magnetic impurities in superconductors has been prominent, recent results with scanning tunneling microscopy of the local density of states of the high- T_c cuprates [2] suggests that a broader range of effects is at play. This includes suppression of the superconducting critical temperature, T_c , by nonmagnetic impurities in superconductors with higher orbital-angular-momentum states such as d states, where impurity scattering blurs the phase assignment for given orientations. An example is Zn substitution for in-plane Cu in $\text{YBa}_2\text{Cu}_3\text{O}_7$ [3] and $\text{Bi}_2\text{Sr}_2\text{CaCu}_2\text{O}_{8+\delta}$ [4]. It also appears that nonmagnetic impurities can produce Friedel oscillations responsible for the striking checkerboard patterns observed near vortex cores [5]. Impurity effects may also inform investigations of pairing mechanisms in high-temperature superconductors [6]. An element missing from this story, which we address here, is a verification of the predictions for nonmagnetic-impurity effects in s -wave superconductors that may underlie more complex phenomena in d -wave materials.

The description of impurities in superconductors begins with the Anderson model of impurity states [7], where a localized transition-metal atom carrying a magnetic moment with a single, intrinsically sharp d -like orbital is embedded in a free-electron gas. Hybridization (resonance) with conduction-electron states leads to a broadening of the d -like density of states (DOS) to an energy width 2Λ , for both spin-up and -down states that have an energy difference of 2ν due to Coulomb repulsion. The impurity remains magnetic if $\pi\Lambda \leq \nu$. Abrikosov and Gorkov (AG) addressed this case in the weak-scattering Born approximation ($\Lambda \ll \nu$) for superconductors [8]. This work was extended by Shiba [9] and Rusinov [10] to include bound states below the gap [11]. Kaiser [12] has addressed the high scattering rate case ($\Lambda \gg \nu$), where the

magnetic moment of the impurity (hereafter referred to as a nonmagnetic impurity) is washed out due to strong coupling to the conduction electrons. A striking difference between the two regimes is revealed in the DOS. For magnetic impurities, any significant suppression of T_c is accompanied by a smearing of the DOS, eventually leading to gapless superconductivity. For nonmagnetic impurities, as T_c and the energy gap are suppressed, a sharp BCS-like density of states is retained. This latter prediction has heretofore gone unobserved.

In this Letter we present tunneling results for Al films doped with Mn. Our results clearly demonstrate T_c suppression, with the retention of the sharp DOS predicted for nonmagnetic Anderson impurities.

We produced Al-Mn alloy thin films on electronic-grade silicon wafers using cosputtering from two adjustable-rate sources, one containing a 99.9995 at. % purity Al target and the other an Al target doped with 3000 ppm Mn, with a stated 99.99 at. % Al purity excluding Mn. Tunnel junctions were prepared from these films as discussed in the context of using Al-Mn as normal-metal electrodes in tunnel refrigerators [13], as with previous work with heavily (1 wt. %) Mn-doped Al [14]. Other general work with Al-Mn alloys has employed vacuum melting [15,16] and ion implantation [17].

To understand the effect of Mn impurities in Al, we first address T_c suppression. As discussed by Arnold [18] a general form for the T_c of a superconductor containing dilute magnetic and nonmagnetic impurities can be written as

$$\beta + \ln\left(\frac{T_c}{T_{co}}\right) + \psi\left(\frac{1}{2} + \frac{\alpha}{2\pi k_B T_c}\right) - \psi\left(\frac{1}{2}\right) = 0, \quad (1)$$

where ψ is the digamma function and T_{co} is the unperturbed critical temperature.

For magnetic impurities only, $\beta = 0$ and T_c is governed by the pair-breaking parameter $\alpha = \frac{\Delta_0}{2} \frac{x}{x_c} [1 - \delta \frac{x}{x_c} \frac{T_{co}}{T_c}]$. This is the AG result where time-reverse symmetry is broken, expressed in the Maki formulation [19], includ-

ing antiferromagnetic Ruderman-Kittel-Kasuya-Yosida (RKKY) coupling [20], where $\delta = \tau_K / \tau_{\text{RKKY}}$, τ_K is the time scale to randomize the relative phase of time-reversed electrons, τ_{RKKY} is the RKKY spin-flip relaxation time, x is the magnetic-impurity concentration, x_c is the critical concentration for which $T_c = 0$ (at $\delta = \beta = 0$), and $\Delta_o = 1.764k_B T_{co}$ is the BCS energy gap.

For nonmagnetic impurities only, $\alpha = 0$ and T_c is governed by $\beta = \frac{1}{\lambda_{\text{eff}}} \frac{n/n_c}{1-n/n_c}$. This is the Kaiser result where n is the nonmagnetic-impurity concentration, n_c is the critical concentration for which $T_c = 0$ (at $\alpha = 0$), and λ_{eff} is an effective electron-phonon coupling parameter. In this case there is no breaking of time-reverse symmetry (pair breaking). Rather, the presence of impurities leads to a local Coulomb repulsion and effective-mass increase that effectively suppress the electron-phonon coupling strength.

Based on these predictions, we can begin to examine whether Mn in Al is acting like a magnetic or nonmagnetic impurity. In Fig. 1 we show results for T_c/T_{co} and low-temperature resistivity $\rho(0) \equiv \rho(4.0 \text{ K})$, versus Mn concentration for Al-Mn. The measured parameters for a test film with 1000 ppm Mn as verified by Rutherford back-scattering were $T_c = 0.437 \text{ K}$ and $\rho(0) = 2.1 \mu\Omega \text{ cm}$, where T_c is defined as the midpoint of the resistive transition. This and subsequent measurement pairs of T_c and $\rho(0)$ at given doping levels were made on sample films

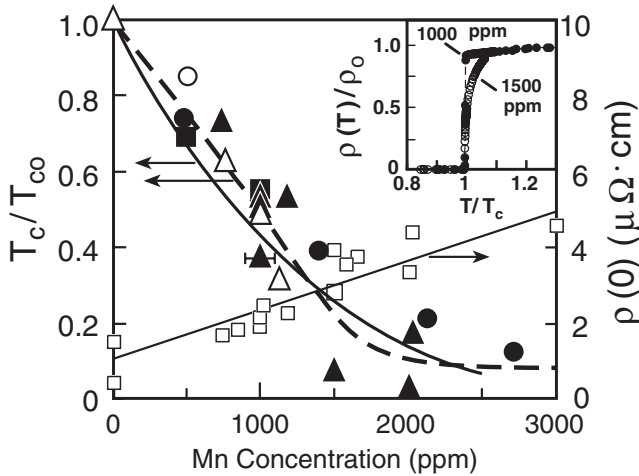


FIG. 1. Reduced critical temperature and low-temperature resistivity versus Mn concentration for Al-Mn alloys from resistive transitions as open circles [17], solid circles [15], and solid squares [16], and our work as solid triangles. Error bar reflects uncertainty based on RBS results. We also include our results from tunnel measurements as open triangles. Also included are results for the Kaiser and Abrikosov-Gorkov theories as solid and dashed lines, respectively. Values of low-temperature resistivity for our work are indicated by open squares. $T_{co} \equiv 1.2 \text{ K}$ and ρ_o is the resistivity just above T_c . Inset shows the resistive transitions for Al-Mn films with 1000 and 1500 ppm Mn [28].

from the same wafers, although T_c measurements were not made on all samples. Films were made and processed separately for transport and tunneling measurements. We observed a $\sim 2\%$ variation of resistivity across a given wafer. Doped samples retained sharp resistive transitions, with a typical width $\Delta T \sim 20 \text{ mK}$ (see inset to Fig. 1). Resistivity ratios $\rho(293 \text{ K})/\rho(4.0 \text{ K}) \geq 3$ were observed for undoped Al films, implying high quality material. We believe we are not in the regime where physical properties, such as disorder-induced effects, influence T_c . This is based on (1) the high resistivity ratios and sharp resistive transitions of our films, (2) the general correspondence between thin-film critical temperatures and those for bulk samples made by vacuum melting, and (3) as discussed below, an energy-gap value for tunnel junctions comprising undoped Al films consistent with a BCS critical temperature $T_c = 1.2 \text{ K}$, the standard bulk value [21].

With the AG model [$\beta = 0$, Eq. (1)], best fits were obtained for $x_c = 1500 \text{ ppm}$ and $\delta = 0.02$. For comparison, $\delta = 0.06$ for W-Fe alloys, in which RKKY effects are believed to have a significant effect on T_c [20]. This value of x_c is large compared with values generally obtained for magnetic impurities. From the same example, $x_c \sim 100 \text{ ppm}$ for Fe in W. For the Kaiser model [$\alpha = 0$, Eq. (1)] a best fit was obtained with $n_c = 9000 \text{ ppm}$ and $\lambda_{\text{eff}} = 0.15$, compared to $\lambda_o = 0.169$ as defined through $T_{co} = 1.13\Theta_D e^{-1/\lambda_o}$, where $T_{co} = 1.2 \text{ K}$ and the Debye temperature $\Theta_D = 394 \text{ K}$ for aluminum [21]. This value of n_c is consistent with values inferred for a variety of nonmagnetic impurities in superconductors, where $n_c \sim 10^4 \text{ ppm}$ [15]. These results suggest that nonmagnetic effects dominate in the reduction of T_c , but do not rule out the participation of magnetic effects.

Tunneling has provided a more definitive description of the Mn impurities. Tunnel measurements for symmetric superconductor/insulator/superconductor systems provide the normalized tunnel conductance $\frac{\sigma(V)}{\sigma_n} = \frac{dI(V)/dV}{(dI(V)/dV)_n}$, where $I(V) = \frac{\sigma_n}{e} \int_{-\infty}^{+\infty} \frac{N(E+eV)N(E)}{N^2(0)} [f(E) - f(E+eV)] dE$, σ_n is the low-temperature normal-state tunnel conductance, $f(E)$ is the usual Fermi function, and V is the bias potential across the junction. For undoped superconductors the DOS is the BCS result $N(E) = N(0) \text{Re} \frac{E}{(E^2 - \Delta_0^2)^{1/2}}$ where $N(0)$ is the normal-state DOS. Here, $N(E)$ is manifest as a sharp peak in $\sigma(V)/\sigma_n$ at a bias $V = 2\Delta_0/e$ for $T \ll T_{co}$.

Both magnetic and nonmagnetic Anderson impurities will modify the DOS in a manner that can be represented by $N(E) = N(0) \text{Re} \frac{E}{[E^2 - \Delta^2(E)]^{1/2}}$. For magnetic impurities any significant suppression of T_c from T_{co} results in a broadening of the peak in the DOS at $E = \Delta_o$, the introduction of states below the gap, and ultimately gapless behavior for $T_c/T_{co} < 0.5$ owing to a strong energy dependence of $\text{Re} \Delta(E)$ and $\text{Im} \Delta(E)$. For nonmagnetic impurities, $\text{Re} \Delta(E) \sim (T_c/T_{co})\Delta_o$ and $\text{Im} \Delta(E)$ enters as a small, localized peak at $E \sim \Delta = (T_c/T_{co})\Delta_o$. This results in the

retention of a BCS-like DOS (where Δ replaces Δ_o) and the absence of states for $E < \Delta$ even for $\Delta \ll \Delta_o$.

In Fig. 2 we show conductance data for Al-Mn junctions with Mn doping levels up to 1200 ppm. The data exhibit sharp, BCS-like peaks and a lack of conductance below the energy gap. In some instances, a weak subgap step (not readily apparent in the figure) is present which we speculate may originate from traces of low-gap or normal material at oxide/metal interfaces. The data were fit and are in good accord with the Kaiser theory for nonmagnetic impurities, shown as the solid lines where Dynes broadening has been included as discussed below. The primary input parameter to the theory is the energy gap defined by the peak in tunnel conductance at $V = 2\Delta/e$. Calculated values of T_c based on $\Delta = 1.764k_B T_c$ were the same as those derived from fitting $\Delta(T)$ (over the range $0.1 < T < 0.6$ K) to weak-coupled BCS theory, within the error reflected by the size of the open triangles in Fig. 1. The T_c calculated for pure Al (0 ppm Mn) is 1.22 K, for a gap of $\Delta = 186 \mu\text{eV}$. We note that the AG theory for magnetic impurities would predict the absence of peak structure for the degree of T_c suppression obtained for all Mn-doped samples, as will be discussed in connection with and detailed in Fig. 3.

Since the width of the peaks is greater than the BCS-like result predicted by the Kaiser model, (and by BCS theory

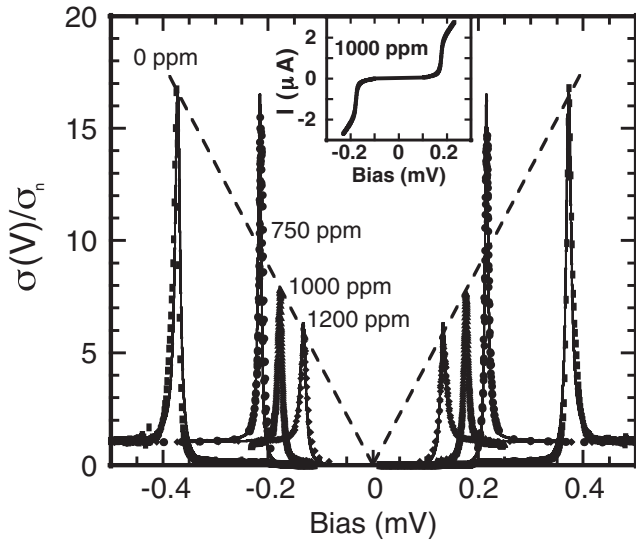


FIG. 2. Normalized tunnel conductance versus bias for Al-Mn/oxide/Al-Mn tunnel junctions with Mn doping concentrations as indicated. All measurements made at $70 < T < 80$ mK. Data are solid symbols and solid lines are fits with the Kaiser theory for nonmagnetic impurities. Dashed lines illustrate the expected linear dependence of peak height with bias, based on the Kaiser model with constant Dynes broadening. Values of the Dynes parameter used to fit the 0, 750, 1000, and 1200 ppm data were $\Gamma = 2.9, 1.75, 3.1$ and $2.9 \mu\text{eV}$, respectively. Inset shows the current-voltage characteristics for the junction with 1000 ppm Mn.

for pure Al junctions) we have included Dynes broadening by introducing an imaginary part, Γ , to the E^2 term (only) in $N(E)$ as $E \rightarrow E + i\Gamma$ [22]. This formulation originates from work addressing lifetime effects in superconductors [23]. We note that the need for such broadening is not unique to this work and has been widely applied to tunnel results for a variety of systems.

The model is consistent with a linearly increasing conductance-peak height for curves of constant width (the 0, 1000, and 1200 ppm data, fit with $\Gamma = 2.9 \mu\text{eV}$), as shown in Fig. 2. We can see this by noting that $[N(\Delta)/N(0)]^2 = \Delta/4\Gamma$ to first order in Γ . This implies that for constant Γ the lines defined by $\sigma(V)/\sigma_n \sim e|V|/8\Gamma$ should give the conductance-peak height for differing gaps. A detailed calculation shows that for the range of parameters here $\sigma(V)/\sigma_n = e|V|/7.7\Gamma$, as plotted for $\Gamma = 2.9 \mu\text{eV}$ (dashed lines). The peak height for the 750 ppm data ($\Gamma = 1.75 \mu\text{eV}$) is also in accord with this model.

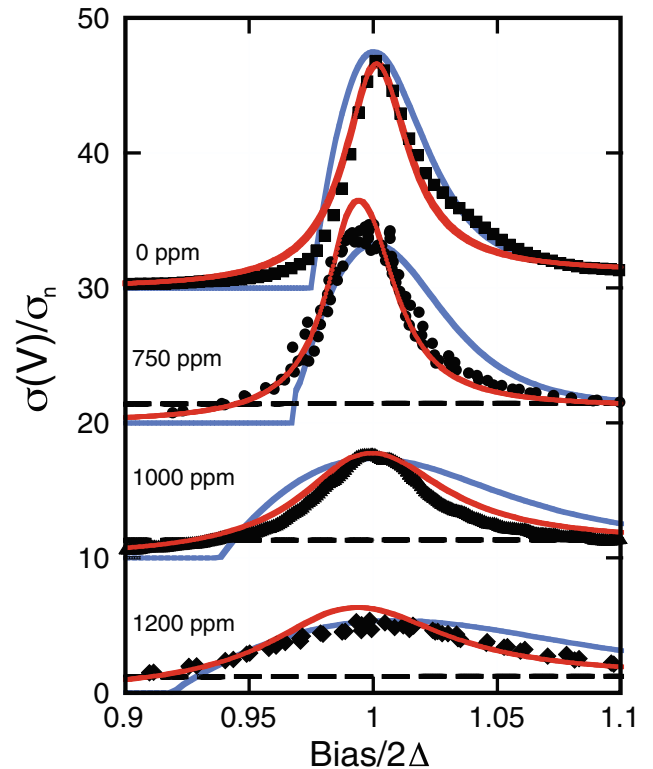


FIG. 3 (color). Normalized conductance versus reduced bias for the data in Fig. 2 (solid symbols), with energy gaps $\Delta = 186, 109, 88.5,$ and $67.0 \mu\text{eV}$ for junctions with Mn concentrations of 0, 750, 1000, and 1200 ppm, respectively. Shown are fits with the Kaiser theory including Dynes broadening from Fig. 2 (here with red lines), and Kaiser theory including magnetic-impurity broadening (blue lines), with values of $2\alpha = 0.8, 0.7, 1.5,$ and $2.0 \mu\text{eV}$ for junctions with Mn concentrations of 0, 750, 1000, and 1200 ppm, respectively. The dashed lines show the Abrikosov-Gorkov result for the case of magnetic Mn impurities. Plots offset by 10 vertical units for clarity.

In Fig. 3 we show detailed fits of the data in the vicinity of the energy gap. Included are fits to the Kaiser theory including Dynes broadening as in Fig. 2 (red lines). We have also separately broadened the peaks by introducing a small quantity of pair breaking $2\alpha = \hbar/\tau_K$ into the Kaiser result to represent possible contamination by magnetic impurities, or a residual magnetic component of the Mn impurities (blue lines). To fit the data, values of $2\alpha \sim 1 \mu\text{eV}$ are required, which is equivalent to $\sim 3 \times 10^{-4}$ at. % (3 ppm) of Fe [16]. This value is within the stated purity of the sputter targets employed and suggests that active magnetic impurities are present at levels not exceeding the equivalent of 6 ppm of Fe in our films. (Preliminary microanalysis indicates that higher concentrations of ferromagnetic contaminants may exist in our Al-Mn targets). In any case, since our control sample with pure Al electrodes (0 ppm Mn) shows a similar degree of broadening as the doped samples (note Fig. 2), this suggests that any small background magnetic effects are not associated with the Mn impurities.

Finally, in Fig. 3 we compare all the conductance data with the AG theory only (dashed lines). This is the model where fully magnetic Mn impurities suppress the energy gap. Clearly, this cannot account for our results, as the gap structure is completely washed out in this case. This analysis taken together implies that there is strong scattering from Mn impurities that lack a discernible magnetic character [24], due to strong mixing with the Al conduction electrons. This is consistent with spin-fluctuation measurements [25] of and the observation of strong resonant-state broadening [26,27] in Al-Mn alloys.

In conclusion, we have investigated the superconducting properties of dilutely doped Al-Mn alloys. We have demonstrated the BCS-like density of states predicted by the Kaiser theory for energy-gap suppression with nonmagnetic Anderson impurities. Our work implies that the Mn impurities have no measurable magnetic character and act exclusively as strong resonant scattering sites without producing time-reverse symmetry breaking of Cooper pairs (pair breaking).

This work has been supported by the Department of Energy.

-
- [1] A. V. Balatsky, I. Vekhter, and J.-X. Zhu, *Rev. Mod. Phys.* **78**, 373 (2006).
 [2] K. M. Lang, V. Madhavan, J. E. Hoffman, E. W. Hudson, H. Eisaki, S. Uchida, and J. C. Davis, *Nature (London)* **415**, 412 (2002).

- [3] K. Ishida, Y. Kitaoka, T. Yoshitomi, N. Ogata, T. Kamino, and K. Asayama, *Physica C (Amsterdam)* **179**, 29 (1991).
 [4] S. H. Pan, E. W. Hudson, K. M. Lang, H. Eisaki, S. Uchida, and J. C. Davis, *Nature (London)* **403**, 515 (2000).
 [5] J. E. Hoffman, E. W. Hudson, K. M. Lang, V. Madhavan, H. Eisaki, S. Uchida, and J. C. Davis, *Science* **295**, 466 (2002).
 [6] K. Terashima, H. Matsui, D. Hashimoto, T. Sato, T. Takahashi, H. Ding, T. Yamamoto, and K. Kadowaki, *Nature Phys.* **2**, 27 (2006).
 [7] P. W. Anderson, *Phys. Rev.* **124**, 41 (1961).
 [8] A. A. Abrikosov and L. P. Gor'kov, *Sov. Phys. JETP* **12**, 1243 (1961).
 [9] H. Shiba, *Prog. Theor. Phys.* **40**, 435 (1968).
 [10] A. I. Rusinov, *Sov. Phys. JETP* **29**, 1101 (1969).
 [11] W. Bauriedl, P. Ziemann, and W. Buckel, *Phys. Rev. Lett.* **47**, 1163 (1981).
 [12] A. B. Kaiser, *J. Phys. C* **3**, 410 (1970).
 [13] A. M. Clark, A. Williams, S. T. Ruggiero, M. L. van den Berg, and J. N. Ullom, *Appl. Phys. Lett.* **84**, 625 (2004).
 [14] D. S. Pyun and T. R. Lemberger, *Phys. Rev. B* **43**, 3732 (1991).
 [15] M. B. Maple, in *Superconductivity in d- and f-Band Metals*, edited by D. H. Douglas AIP Conf. Proc. (AIP, New York, 1971), Vol. 4, p. 175.
 [16] G. Boato, G. Gallinaro, and C. Rizzuto, *Phys. Rev.* **148**, 353 (1966).
 [17] B. A. Young, J. R. Williams, S. W. Deiker, S. T. Ruggiero, and B. Cabrera, *Nucl. Instrum. Methods Phys. Res., Sect. A* **520**, 307 (2004).
 [18] G. B. Arnold, *Phys. Rev. B* **10**, 105 (1974).
 [19] K. Maki, in *Superconductivity*, edited by R. D. Parks (Marcel Dekker, New York, 1964), p. 1035.
 [20] B. A. Young, T. Saab, B. Cabrera, J. J. Cross, R. M. Clarke, and R. A. Abusaidi, *J. Appl. Phys.* **86**, 6975 (1999).
 [21] N. W. Ashcroft and N. D. Mermin, *Solid State Physics* (Saunders College, Philadelphia, 1976), 1st ed.
 [22] R. C. Dynes, V. Narayanamurti, and J. P. Garno, *Phys. Rev. Lett.* **41**, 1509 (1978).
 [23] S. B. Kaplan, C. C. Chi, D. N. Langenberg, J. J. Chang, S. Jafarey, and D. J. Scalapino, *Phys. Rev. B* **14**, 4854 (1976).
 [24] F. W. Smith, *J. Low Temp. Phys.* **6**, 435 (1972).
 [25] E. Babic, R. Krsnik, B. Leontic, Z. Vucic, I. Zoric, and C. Rizzuto, *Phys. Rev. Lett.* **27**, 805 (1971).
 [26] B. D. Terris and D. M. Ginsberg, *Phys. Rev. B* **27**, 1619 (1983).
 [27] Y. Okabe and A. D. S. Nagi, *Phys. Rev. B* **28**, 2455 (1983).
 [28] S. T. Ruggiero, A. Williams, W. H. Rippard, A. Clark, S. W. Deiker, L. R. Vale, and J. N. Ullom, *J. Low Temp. Phys.* **134**, 973 (2004).